Intensity clamping measurement of laser filaments in air at 400 and 800 nm

J.-F. Daigle,[1] A. Jaroń-Becker,[2] S. Hosseini,[1] T.-J. Wang,[1] Y. Kamali,[1] G. Roy,[3] A. Becker,[2] and S. L. Chin[1]

[1]*Centre d'Optique, Photonique et Laser (COPL) and Département de Physique, de Génie Physique et d'Optique, Université Laval, Québec, Québec G1V 0A6, Canada*

[2]*JILA and Department of Physics, University of Colorado, Boulder, Colorado 80309–0440, USA*

[3]*Defence Research and Development Canada-Valcartier, 2459 Pie-XI Boulevard North, Québec, Québec G3J 1X5, Canada*

Molecular N_2 fluorescence excited by laser filaments formed from laser pulses at 400 and 800 nm propagating in air is investigated. A comparison showed that, when excited with 400 nm photons, the fluorescence from the first negative band of N_2^+ was enhanced by a factor of 6.4 while that of the second positive band of neutral N_2 remained relatively constant. The enhanced N_2^+ signal is attributed to a more efficient *inner-shell* multiphoton process (to the $B\,^2\Sigma_u^+$ state) at 400 nm leaving a larger population of N_2^+ ions in the excited state. On the other hand, the stable fluorescence from neutral N_2 is due to the fact that the plasma density is more or less the same at both wavelengths. Using these results, a theoretical model is developed to determine the clamped intensities of the laser filaments at 400 and 800 nm.

PACS number(s): 33.80.Rv, 52.50.Jm, 42.62.Fi

I. INTRODUCTION

In the last decade, there has been a growing interest in the formation of long plasma channels by high-power femtosecond laser pulses propagating in air. Nowadays, these long plasma channels are better known by the name filaments [1–6]. Because of their remarkable properties (remote projection of high laser intensity [7], km-range plasma channels [8], and spectral broadening due to self-phase modulation [9]), filaments have attracted a lot of interest in the scientific community regarding remote atmospheric applications [4]. Numerous proposals range from remote sensing of atmospheric constituents [10] to remote generation of THz waves in air [11].

In air, filaments primarily appear due to a dynamic equilibrium between Kerr self-focusing and defocusing by the self-generated low-density plasma produced by multiphoton or tunnel ionization of the air molecules [1,6]. Indeed, for a nonuniform laser intensity distribution (Gaussian, for example) with peak power higher than the critical power for self-focusing, the Kerr effect will act as a lens that will focus the light pulse until its intensity is sufficiently high to ionize the medium in which it propagates. Once the plasma is sufficiently dense to counteract the Kerr lens effect, the laser pulse will start to defocus. The defocusing nature of the plasma limits and stabilizes the light intensity in each of the filaments (intensity clamping). In air, for 800 nm of laser light, the clamped intensity is approximately 5×10^{13} W/cm^2 [12,13] and is sufficiently high to ionize any atmospheric constituent or contaminant.

Because of the lack of sources providing powerful pulses at different wavelengths, most of the experimental and theoretical works on filamentation in air have been performed at 800 nm, the central wavelength of the Ti:sapphire gain medium. At this wavelength, energetically speaking, a minimum of 8 photons is required to ionize O_2 and a minimum of 11 photons to obtain ionized N_2, establishing the detection threshold intensity for ionization of air around 10^{13} W/cm^2. It is possible, by using laser pulses with more energetic photons, to reduce this threshold and increase the ionization

efficiency of the laser pulse. Indeed, at the same intensity the ionization probability of a medium is enhanced significantly as the wavelength decreases, thus increasing the probability of plasma filaments' formation.

While filamentation at Ti:sapphire wavelengths (of about 800 nm) has been studied thoroughly over the last years, there has been much less effort dedicated to filamentation of uv laser pulses (e.g., [14–17]). For example, filaments obtained from uv pulses propagating in air were observed at a distance of 12 m from the source with an estimated intensity of $\sim 3 \times 10^{12}$ W/cm^2 and an electron density of $\sim 10^{16}$ cm^{-3} [14]. Recently Zhang *et al.* [18] characterized laser filaments at 400 nm formed from prefocused and collimated laser pulses and measured the plasma column diameter and the electron density. For laser pulses focused with a 1-m-focal-length lens, the measured plasma density was $\sim 2 \times 10^{17}$ cm^{-3}, which is larger by more than an order of magnitude than the results of previous measurements. Moreover, in the collimated regime, they observed multiple filaments over a distance of 70 m.

After filamentation in air, the plasma left behind undergoes complex transitions to emit characteristic, fingerprint fluorescence [6,10]. For filamentation in air and nitrogen gas, fluorescence bands attributed to N_2^+ and N_2 have been observed (the N_2 energy diagram is presented in Fig. 1). The fluorescence from the first negative band system ($B\,^2\Sigma_u^+ - X\,^2\Sigma_g^+$ transition) of N_2^+ in the plasma filament results from intense laser-induced multiphoton or tunnel ionization of inner-valence electrons of neutral nitrogen molecules, leaving the molecular ion N_2^+ in the excited state $B\,^2\Sigma_u^+$ [19–21]. The mechanism linked to the neutral fluorescence of N_2's second positive band is not so straight forward. The $C\,^3\Pi_u$ energy level of N_2 cannot be directly populated from the ground state because of the forbidden singlet- to triplet-state transition. Moreover, because of insufficient energy of the emitted electron at rather low laser intensities, the population of $C\,^3\Pi_u$ via inelastic collision with electrons is highly unlikely. Xu *et al.* proposed a model where the primary reaction $N_2^+ + N_2 = N_4^+$ followed by the recombination with an electron is responsible for populating the electronic excited level $C\,^3\Pi_u$ of N_2 [22].
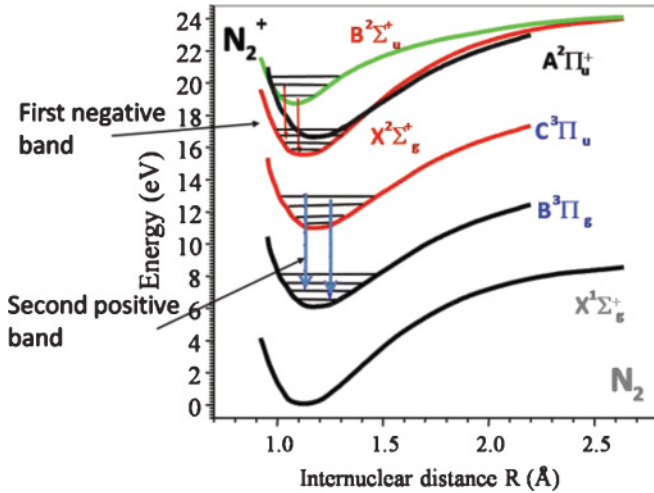
FIG. 1. (Color online) N_2 molecule energy diagram. The first negative band of N_2^+ corresponds to the transition $B\,^2\Sigma_u^+ - X\,^2\Sigma_g^+$, whereas the second positive band of N_2 corresponds to the transition $C\,^3\Pi_u - B\,^3\Pi_g$.

In this work, filaments, obtained from the propagation of 400-nm short laser pulses in air, are studied via the fluorescence from the excited neutral N_2 molecules and the N_2^+ ions. Compared to filaments generated at 800 nm, the fluorescence signal from the first negative band of N_2^+ is significantly enhanced (by a factor ~ 6.4), whereas the one corresponding to the neutral excited N_2 remains practically unchanged. Based on a theoretical analysis of these data, we propose a method to determine the clamped intensities inside the filaments at both wavelengths.

II. EXPERIMENTAL SETUP

Amplified laser pulses, emitted at a 10-Hz repetition rate from a typical chirped pulse amplification (CPA) laser system, were compressed near the experimental setup with a portable grating compressor. The pulses, after compression, were characterized with a maximal energy of 13 mJ and a transform-limited pulse duration of 42 fs. The spectrum was centered at 800 nm and had a 23 nm spectral width full width at half maximum (FWHM).

A 100-μm-thick beta barium borate (BBO) crystal with a 10-mm clear aperture was used for up-frequency conversion to obtain the desired 400-nm wavelength. Two dichroic mirrors with high reflectivity at 400 nm were used to filter out the fundamental beam. The pulse energy, after the two dichroic mirrors, was 2.3 mJ. The spectrum of the blue pulses was centered at 400 nm with a width of 4 nm FWHM. Assuming a transform-limited Gaussian pulse distribution, we obtain, from the time-bandwidth product, a minimum pulse duration of 59 fs.

N_2 fluorescence generated by laser filaments produced from 800-nm pulses was also investigated. To do so, the BBO crystal was removed and the two dichroic mirrors were replaced by dielectric mirrors with high reflectivity at 800 nm. In order to compare 400- and 800-nm filaments, the pulse energy at both wavelengths was fixed to 2.3 mJ. The laser pulses were then focused in air with a 15-cm-focal-length
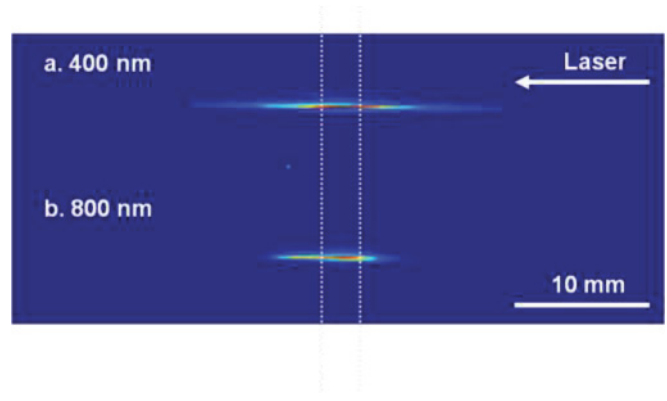

FIG. 2. (Color online) Fluorescence signal distribution of laser filaments obtained from 2.3-mJ laser pulses at 400 and 800 nm. The CCD camera was protected with a UG11 bandpass filter and two dielectric mirrors with high reflection at 400 and 800 nm. The vertical dotted lines correspond to the 3-mm-long signal portion incident on the fiber bundle.

lens. The fluorescence spectra from N_2 were measured using a fiber bundle connected to an imaging spectrometer coupled to a gated intensity charge-coupled device (ICCD). A 10-cm-focal-length lens was used in a 4f configuration to image the characteristic N_2 fluorescence, emitted by a 3-mm-long section of the filament zone, onto the 3-mm-wide aperture of a fiber bundle's collecting lens. Figure 2 shows the filaments' spatial distribution (fluorescence) collected from the side by a charge-coupled device (CCD) camera for 400- and 800-nm laser pulses. The camera objective was protected with a UG11 filter, transmitting only N_2 and N_2^+ fluorescence, and two dielectric mirrors, one with high reflection at 800 nm and the other at 400 nm. Each picture was accumulated over 600 laser shots. The two dotted lines indicate the filament region from which the fluorescence signal has been collected by the fiber bundle. From the results we assume a cylindrically symmetric intensity distribution inside the filament, that is, a constant intensity along the propagation direction and a Gaussian distribution in the transverse direction. The transverse extension of the filament (measured at e^{-2} of the maximum signal value) was about 1.25 times larger for filamentation of the 800-nm pulse as compared to that for filamentation of the 400-nm pulse. For further analysis, the fluorescence spectra have been normalized to the same interaction volume.

III. EXPERIMENTAL RESULTS AND ESTIMATION OF THE PLASMA DENSITY

Figure 3 presents typical N_2 spectra collected for the filamentation of 800-nm (black curve) and 400-nm (gray curve) laser pulses. Both traces are normalized to the intensity of the strongest emission band for filaments at 400 nm. The ICCD's time gate started 2 ns before the laser pulses formed the filaments and was opened for 20 ns. The spectra were accumulated for five laser shots. Under these conditions, the normalized fluorescence signal from the first negative band of N_2^+ is enhanced by a factor 6.4 for laser filaments at 400 nm as compared to those at 800 nm. We attribute this
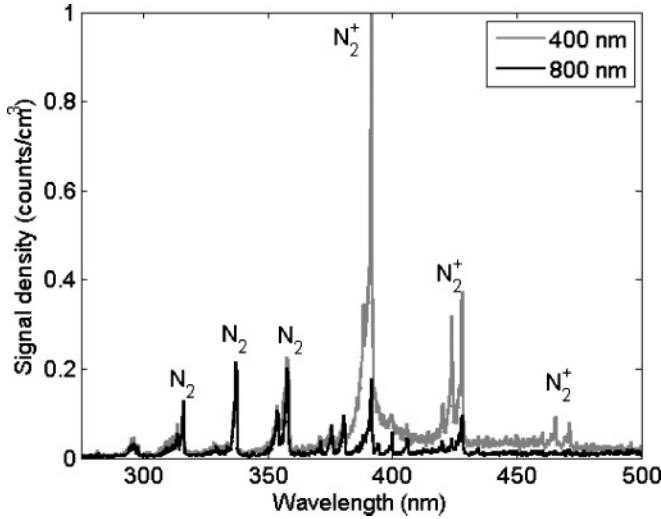
FIG. 3. Typical fluorescence spectra obtained from laser filaments in air and normalized to the same interaction volume for $\lambda = 800$ nm (black) and $\lambda = 400$ nm (gray). In both situations the pulse energy is 2.3 mJ. The two traces are normalized to the strongest emission band obtained for filaments at 400 nm. At 400 nm, fluorescence from the first negative band is enhanced by a factor ∼6.4, whereas signals from the second positive band seem to be wavelength independent.

enhanced signal to a more efficient *inner-shell* multiphoton process (to the $B\,^2\Sigma_u^+$ state) at 400 nm leaving a larger population of N_2^+ ions in the excited state. On the other hand, the fluorescence signal from the excited neutral N_2 is almost the same for the two wavelengths. According to the model by Xu *et al.* [22] the excited state in the neutral nitrogen molecules is populated via collisions between neutral and ionic molecules, followed by electron recombination. Thus, the unchanged fluorescence signals from excited neutral N_2 molecules at different wavelengths indicate that the *total* ionization yield, which is proportional to the population of the excited neutral molecules, is the same for filamentation at 400 and 800 nm. The near equality of the total yield can be understood as a consequence of intensity clamping. Indeed, because the Kerr nonlinear index of refraction for the two wavelengths does not change much, the plasma required to balance any change of the Kerr index should not change much either. Literature data for the Kerr nonlinear index are 3×10^{-19} cm^2/W ($\lambda = 800$ nm) and 8×10^{-19} cm^2/W ($\lambda = 248$ nm) [23], we may expect that the value for $\lambda = 400$ nm is in this range too. Hence, we assume an approximate value of n_2 for 400 nm to be 4×10^{-19} cm^2/W for the following estimation.

Neglecting the effects of external focusing, this estimation can be done using Drude's model to calculate the refractive index change attributed to the formation of the plasma (Δn_{plasma}). It is defined as

$$\Delta n_{\text{plasma}} = -\frac{N_e e^2}{2 s_D m_e \omega_0^2}, \qquad (1)$$

where N_e corresponds to the plasma density, e is the elementary charge, m_e is the mass of the electron, ε_0 is the vacuum permittivity, and ω_0 is the pulse's central angular frequency.

TABLE I. Plasma densities calculated using Eq. (2) for $\lambda = 248$, 400, and 800 nm.

Wavelength (nm)	Nonlinear index n_2 (cm^2/W)	Clamped intensity I (W/cm^2)	Plasma density N_e (cm^{-3})
248	8×10^{-19}	3×10^{12}	8.7×10^{16}
400	4×10^{-19}	1.5×10^{13}	8.4×10^{16}
800	3×10^{-19}	5×10^{13}	5.2×10^{16}

During filamentation, Δn_{plasma} balances the refractive index change attributed to Kerr self-focusing, defined as $\Delta n_{\text{Kerr}} = n_2 I$, where n_2 is the air nonlinear index of refraction and I is the clamped intensity. The plasma density can therefore be retrieved from the relation

$$N_B = \frac{2 s_0 m_e \omega_0^2 n_2 I}{e^2}. \qquad (2)$$

The plasma density is computed at three different wavelengths, 248, 400, and 800 nm. The results are presented in Table I. Even though these results are approximations, the plasma density does not change much over this spectral range. The observation of a near equality of the total ionization yield is also in agreement with the results of numerical calculations by Couairon and Bergé [23], who have found that, for fixed focusing conditions, the plasma density generated by infrared and uv filaments is more or less the same. It is fair to deduce that it is also the case for 400-nm laser filaments.

IV. THEORETICAL MODEL: DETERMINATION OF CLAMPED INTENSITIES

Next, we use these observations to obtain an estimate of the clamped (peak) intensities inside the filaments at 400 and 800 nm. To this end, let us summarize our previous conclusions into two experimentally observed conditions.

(1) The *total ionization yields* inside the filaments generated by 400- and 800-nm laser pulses (with same input energy) are the same.

(2) The partial *inner-shell ionization yield* (to the $B\,^2\Sigma_u^+$ state in the N_2^+ ion) inside the filaments is 6.4 times larger when using 400-nm pulses as compared to using 800-nm pulses.

These conditions are formulated in terms of the (partial or total) ionization yields. Since the yields depend dominantly on the peak intensity of the pulses inside the filament, both conditions provide two relations to determine the two unknown clamped (peak) intensities inside the two filaments at 400 and 800 nm.

In order to determine the clamped intensities we have performed calculations of the rates of ionization of N_2 to the ground and the excited states of the ion using the strong-field S-matrix theory [15,24]. Then, we have obtained the ionization yields in the interaction volume for the ensemble of molecules in the filament using the rate equations [25]. For the present calculations we considered a cylindrical interaction volume with a constant intensity distribution along the propagation axis and a Gaussian intensity distribution perpendicular to it. We further considered Gaussian temporal distributions with
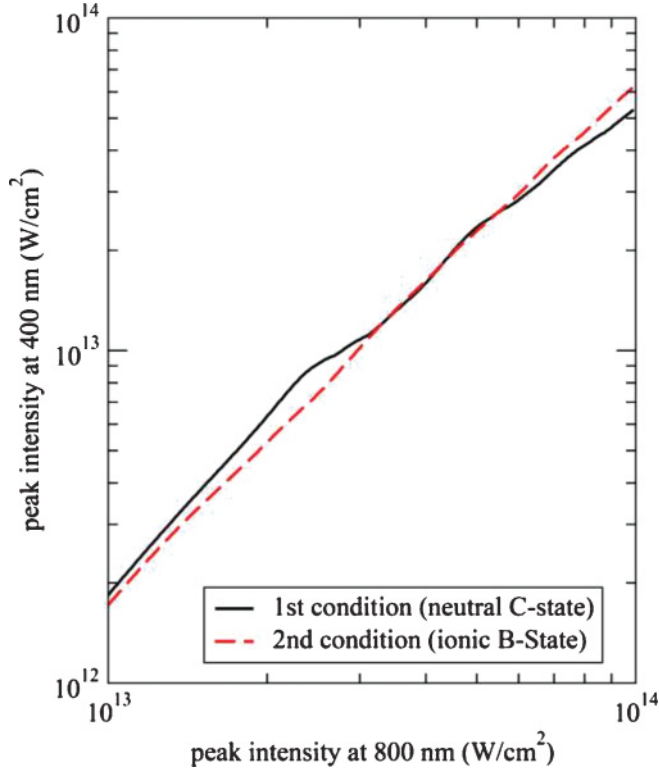
FIG. 4. (Color online) Pairs of intensities at which either condition 1 (equality of the total ion yields, black curve) or condition 2 (enhancement of the partial inner-shell ion yield at 400 nm, dashed curve) is fulfilled. The range for the clamped intensities is determined in the zone where both conditions are respected, that is, at the crossing point.

different pulse durations (10–45 fs, FWHM, for λ = 800 nm, and 10–59 fs, FWHM, for λ = 400 nm). We found that the results for the clamped intensities, presented subsequently, do not depend much on the temporal and spatial intensity distribution (by less than 10% for the actual parameters considered here).

From the ion yields, we determined those pairs of intensities at which either condition 1 (equality of the total ion yields) or condition 2 (enhancement of the partial inner-shell ion yield at 400 nm) is fulfilled. These results are plotted in Fig. 4 as black (condition 1) and dashed curves (condition 2), respectively. The clamped intensities can be determined if both conditions are fulfilled, that is, at the crossing points of the two curves. From Fig. 4 we see that the two curves cross over a regime of intensities, clamped intensities, ranging between $(3–5.5) \times 10^{13}$ W/cm^2 for λ = 800 nm and $(1–2.5) \times 10^{13}$ W/cm^2 for λ = 400 nm. The former result at 800 nm is actually in agreement with the results of previous observations and numerical estimates [12,13,24].

One would expect that both conditions are fulfilled over a rather narrow intensity regime only, which would let us determine the clamped intensities very accurately. From the results presented in Fig. 4 we, however, see that this is not the case for the present analysis, since both curves are almost parallel and the black curve, which corresponds to the equality of the total ionization yields, is very wavy. The latter feature is a signature of pronounced channel-closing effects, which result

in a drop of the ionization rate at certain intensities.[1] Due to the average over the temporal and spatial intensity profiles these effects are usually not present in the ion yields. For molecular ionization from σ_g orbitals, channel-closing effects are, however, found to be very pronounced [25], such that they even appear as variations in the ion yields. Since the total ionization yields for N$_2$ are dominantly due to emission of an electron from the highest occupied molecular orbital, which is of σ_g symmetry, the black curve is quite wavy. On the other hand, the partial inner-shell ionization yields (condition 2) correspond to ionization of an electron from a σ_u orbital, for which the channel-closing effects are less pronounced. This leads to the rather straight red curve in Fig. 4.

It remains to clarify the almost parallel gradients of the two curves in Fig. 4. To this end, we may remind the reader that laser-induced ion-yield curves as a function of intensity do often scale by a power law. Thus, condition 1 reads as

$$A I_{400}^{n_x} = B I_{800}^{m_x},$$

while condition 2 is given by

$$C I_{400}^{n_b} = 6.4 D I_{800}^{m_b}.$$

The first equation shows that I_{400} has to change by a factor of $2^{m_x/n_x}$ if I_{800} is changed by a factor of 2 for the equation to hold. Thus, the gradient of the black curve (condition 1) in Fig. 4 is determined by m_x/n_x. Analogously, the gradient of the dashed curve (condition 2) is determined by m_b/n_b. The exponents m_x, m_b, n_x, and n_b in the power laws are usually not exactly given by, but are related to, the minimum number of photons required to be absorbed from the field to ionize the electron from the corresponding orbital. Thus, we expect that m_b and m_x differ by about 2, since it needs two photons less to ionize N$_2$ to the ground state of the ion than to its B state using 800-nm photons. For 400 nm, one photon more is needed to ionize N$_2$ to the B state of the ion than to the ionic ground state. Thus, n_b and n_x should differ by about 1 unit. Consequently,

$$\frac{m_b}{n_b} \simeq \frac{m_x + 2}{n_x + 1}$$

and, hence, the gradients of the two curves are similar.

With the present method the clamped intensities for filaments at two wavelengths can be obtained at the same time. We note that the method does *not* require that the total ionization yields (condition 1) be the same for both wavelengths. In fact, they may differ by a factor, like the partial ionization yields (condition 2) in the present case. Furthermore, the method is not restricted to filamentation in N$_2$ (or air); any other target gas can be used too, as long as the yields of two transitions (here, ionization to different states) can be obtained in experiment as well as in theory. From the present results we may conclude that any channel-closing

---

[1]The minimum number of photons required to ionize the molecule depends on the quiver energy $Up = I/4\omega^2$ (in Hartree atomic units), where ω is the frequency of the laser. Thus, with an increase in the intensity, the minimum number of photons increases stepwise by 1 unit. This effect is called channel closing.

effects should best be avoided, for example, by choosing ionization from π orbitals, which show less pronounced channel closings [25]. Furthermore, the gradients of the different yields as a function of intensity should differ as largely as possible. This can usually be achieved by a large difference in the ionization potentials and/or a large difference in the two wavelengths.

V. CONCLUSION

In this article, we have investigated the molecular N_2 characteristic fluorescence emitted by laser filaments produced from laser pulses at 400 and 800 nm. A comparison revealed that, with $\lambda = 400$ nm, the first negative band of N_2^+ is enhanced by a factor of 6.4, whereas the second positive band of neutral N_2 is almost the same at both wavelengths. The enhanced N_2^+ signal is attributed to a more efficient inner-shell multiphoton process (to the $B\,^2\Sigma_u^+$ state) at 400 nm leaving a larger population of N_2^+ ions in the excited state, whereas the stable fluorescence from neutral N_2 is due to

the fact that the plasma density is more or less the same at both wavelengths. Using these results, a theoretical model was developed to determine the clamped intensities of the laser filaments at 400 and 800 nm based on two experimentally observed conditions.

(1) The *total ionization yield* is constant at both wavelengths.

(2) The partial *inner-shell ionization yield* (to the $B\,^2\Sigma_u^+$ state in the N_2^+ ion) inside the filaments at 400 nm is 6.4 times larger than that inside the filaments at 800 nm.
Using this method, the obtained clamped intensities range between $(3–5.5) \times 10^{13}$ W/cm^2 for $\lambda = 800$ nm and $(1–2.5) \times 10^{13}$ W/cm^2 for $\lambda = 400$ nm.

[1] S. L. Chin, S. A. Hosseini, W. Liu, Q. Luo, F. Theberge, N. Aközbek, A. Becker, V. P. Kandidov, O. G. Kosareva, and H. Schroeder, Can. J. Phys. **83**, 863 (2005).

[2] A. Couairon and A. Mysyrowicz, Phys. Rep. **441**, 47 (2007).

[3] L. Bergé, S. Skupin, R. Nuter, J. Kasparian, and J.-P. Wolf, Rep. Prog. Phys. **70**, 1633 (2007).

[4] J. Kasparian and J.-P. Wolf, Opt. Express **16**, 466 (2008).

[5] V. P. Kandidov, S. A. Shlenov, and O. G. Kosareva, Quantum Electron. **39**, 205 (2009).

[6] S. L. Chin, *Femtosecond Laser Filamentation* (Springer, New York, 2010).

[7] J.-F. Daigle, Y. Kamali, J. Bernhardt, W. Liu, C. Marceau, A. Azarm, and S. L. Chin, Opt. Commun. **281**, 3327 (2008).

[8] M. Rodriguez *et al.*, Phys. Rev. E **69**, 036607 (2004).

[9] F. Théberge, W. Liu, Q. Luo, and S. L. Chin, Appl. Phys. B **80**, 221 (2005).

[10] S. L. Chin *et al.*, Appl. Phys. B **95**, 1 (2009).

[11] C. D'Amico, A. Houard, M. Franco, B. Prade, A. Mysyrowicz, A. Couairon, and V. T. Tikhonchuk, Phys. Rev. Lett. **98**, 235002 (2007).

[12] J. Kasparian, R. Sauerbrey, and S. L. Chin, Appl. Phys. B **71**, 877 (2000).

[13] A. Becker, N. Akozbek, K. Vijayalakshmi, E. Oral, C. M. Bowden, and S. L. Chin, Appl. Phys. B **73**, 287 (2001).

[14] J. Schwarz, P. Rambo, J. C. Diels, M. Kolesik, E. Wright, and J. Moloney, Opt. Commun. **180**, 383 (2000).

[15] B. Prade, M. Franco, A. Mysyrowicz, A. Couairon, H. Buersing, B. Eberle, M. Krenz, D. Seiffer, and O. Vasseur, Opt. Lett. **31**, 2601 (2006).

[16] P. Bejot, C. Bonnet, V. Boutou, and J. P. Wolf, Opt. Express **15**, 13295 (2007).

[17] O. Chalus, A. Sukhinin, A. Aceves, and J. C. Diels, Opt. Commun. **281**, 3356 (2008).

[18] Z. Zhang, X. Lu, T.-T. Xi, W. X. Liang, Z.-Q. Hao, Y. Zhang, M.-L. Zhou, Z.-H. Wang, and J. Zhang, Appl. Phys. B **97**, 207 (2009).

[19] G. N. Gibson, R. R. Freeman, and T. J. McIlrath, Phys. Rev. Lett. **67**, 1230 (1991).

[20] A. Talebpour, S. Petit, and S. L. Chin, Opt. Commun. **171**, 285 (1999).

[21] A. Becker, A. D. Bandrauk, and S. L. Chin, Chem. Phys. Lett. **343**, 345 (2001).

[22] H. L. Xu, A. Azarm, J. Bernhardt, Y. Kamali, and S. L. Chin, Chem. Phys. **360**, 171 (2009).

[23] A. Couairon and L. Bergé, Phys. Rev. Lett. **88**, 135003 (2002).

[24] J. Muth-Böhm, A. Becker, and F. H. M. Faisal, Phys. Rev. Lett. **85**, 2280 (2000).

[25] A. Jaroń-Becker, A. Becker, and F. H. M. Faisal, Phys. Rev. A **69**, 023410 (2004).